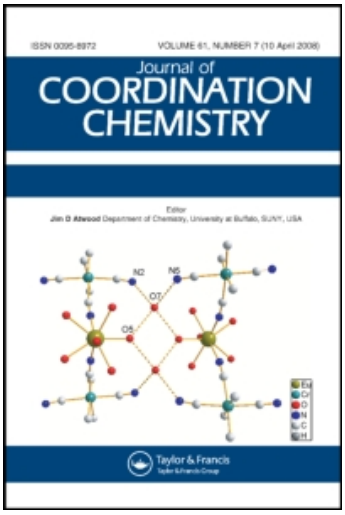


## Journal of Coordination Chemistry

Publication details, including instructions for authors and subscription information:
http://www.informaworld.com/smpp/title~content=t713455674

# Synthesis and characterization of heterooligonuclear ruthenium complexes with tri(phenanthrolino)hexaazatriphenylene ligands

T. David Pilz[a]; Nils Rockstroh[a]; Sven Rau[ab]
[a] Institute of Inorganic and Analytical Chemistry, Friedrich-Schiller-Universität-Jena, Jena, Germany [b] Department of Chemistry and Pharmacy, Friedrich-Alexander-Universität Erlangen-Nürnberg, Erlangen, Germany

Online publication date: 16 August 2010

**To cite this Article** David Pilz, T. , Rockstroh, Nils and Rau, Sven(2010) 'Synthesis and characterization of heterooligonuclear ruthenium complexes with tri(phenanthrolino)hexaazatriphenylene ligands', Journal of Coordination Chemistry, 63: 14, 2727 — 2742
**To link to this Article: DOI:** 10.1080/00958972.2010.508517
**URL:** http://dx.doi.org/10.1080/00958972.2010.508517

*Journal of Coordination Chemistry*
Vol. 63, Nos. 14–16, 20 July–20 August 2010, 2727–2742



# Synthesis and characterization of heterooligonuclear ruthenium complexes with tri(phenanthrolino)hexaazatriphenylene ligands

T. DAVID PILZ†, NILS ROCKSTROH† and SVEN RAU*†‡

†Institute of Inorganic and Analytical Chemistry, Friedrich-Schiller-Universität-Jena, Jena, Germany
‡Department of Chemistry and Pharmacy, Friedrich-Alexander-Universität Erlangen-Nürnberg, Erlangen, Germany

(*Received 19 January 2010; in final form 23 June 2010*)



A homologous series of homo- and heterooligonuclear ruthenium/palladium complexes of 9,10,19,20,29,30-hexaazahexapyrido[3,2-a:2′,3′-c:3″,2″-k:2‴,3‴-m:-3⁗,2⁗-u:2⁗′,3⁗′-w]-trinaphthylene (PHAT) with the formula $[\{Ru(tbbpy)_2\}_n(\mu\text{-phat})]^{2n+}$ $(n=1,2,3)$ and $[\{Ru(tbbpy)_2\}_m(\mu\text{-phat})\{PdCl_2\}_{3-m}]^{2m+}$ $(m=1,2)$ was prepared and characterized, where TBBPY = 4,4′-di-*tert*-butyl-2,2′-bipyridine. Toward this aim, a new synthetic route was developed for which a microwave-assisted successive complexation reaction of the multitopic ligand was used. In accordance to the only known complex of this kind, $[\{Ru(phen)_2\}_3(\mu\text{-phat})]^{6+}$, only the outer 1,10-phenanthroline (PHEN) like coordination spheres of the ligand could be substituted with octahedral ruthenium and square planar palladium fragments. This allows the construction of new supramolecular structures with at least three metal centers that are potentially capable of intramolecular multielectron transfer and photocatalytic redox activity. Electrochemical investigations show that the metal centers in the homonuclear ruthenium complex do not interact and that the ligand-based redox steps are reversible. Preliminary investigations also show that PHAT may be photochemically reduced as seen by UV-Vis spectroscopy; however, no catalytic activity for photochemical hydrogen production could be observed.

*Keywords*: Ruthenium; Palladium; PHAT complexes; Supramolecular chemistry; Photocatalysis

## 1. Introduction

Heteronuclear ruthenium polypyridine complexes have attracted considerable attention in recent years because of their ability to act as supramolecular devices in light-driven catalysis [1–4]. In such supramolecular devices, $[Ru(bpy)_3]^{2+}$ like substructures act as a chromophore in the visible region and as single electron donors with exceptional chemical stability and photophysical properties [5]. The combination of these ruthenium fragments with catalytically active metals, such as palladium, rhodium, or platinum interconnected *via* bridging ligands was successfully used to build up intramolecular catalysts for photoinduced hydrogen evolution [1–3, 6]. One of these

*Corresponding author. Email: sven.rau@chemie.uni-erlangen.de


ISSN 0095-8972 print/ISSN 1029-0389 online © 2010 Taylor & Francis
DOI: 10.1080/00958972.2010.508517

systems contains a $[Ru(tbbpy)_2]^{2+}$ photocenter, a tetrapyrido[3,2-a:2′,3′-c:3″2″-h:2‴3‴-j]-phenazine (TPPHZ) bridging ligand and a $[PdCl_2]$ unit, serving as catalytic center [3]. Detailed mechanistic investigations suggest that the phenazine moiety of the TPPHZ bridge plays an essential role as electron storage moiety for the catalytic process [3]. The bridging ligand also seems to allow for ultrafast electron transfer events to take place [7]. MacDonnell and coworkers [8, 9] showed that a related bi-chromophoric complex with the extended ligand, namely, TATPP (9,11,20,22-tetraazatetrapyrido-[3,2-a:2′,3′-c:3″,2″-l:2‴,3‴-n]-pentacene) is capable of reversibly storing two electrons on the pentacene moiety upon irradiation with visible light.

Toward the aim of combining more than one photochemically active metal center with one catalytically active center one can use dendrimers to build up a light-harvesting unit [10]. Brewer *et al*. [1] have shown that a supramolecular photocatalyst consisting of two ruthenium complexes bound to one rhodium center produces hydrogen upon irradiation with visible light. Here, two bridging ligands, carrying ruthenium centers, occupy four coordination sites of the octahedral rhodium center, thereby limiting the number of accessible coordination sites during catalytic conversion. Based on these two observations, we here aim at a bridging ligand structure which is capable of binding more than two metal centers, but blocks fewer coordination sites at the catalytic metal center and contains a phenazine-like substructure. Within this context, the use of 9,10,19,20,29,30-hexaazahexapyrido[3,2-a:2′,3′-c:3″,2″-k:2‴,3‴-m:-3⁗,2⁗-u:2⁗⁗,3⁗⁗-w]trinaphthylene (PHAT) as potential bridging ligand, combining multichromophore and multielectron storage strategies, seems interesting. To the best of our knowledge, only homotrinuclear ruthenium complexes, containing the PHAT ligand, have been prepared by Lehn *et al*. [11] and later by MacDonnell *et al*. [12] following a different strategy.

The use of the planar PHAT molecule with its extended $\pi$-system comes along with several problems. In the PHAT molecule, two different kinds of binding sites exist (figure 1). There are three inner hexaaminotriazine (HAT)-like diazadiene coordination spheres which are easily accessible for small metal centers with little steric requirements and preferential tetrahedral geometry (depicted as free coordination spheres) [14]. There are also three outer phenanthroline-like coordination pockets, potentially accessible for sterically demanding metal fragments, such as octahedral ruthenium and square planar palladium(II) centers (figure 1). These structural properties raise the question of regioselectivity of the metal coordination. Another problem is the general insolubility of the PHAT molecule in common solvents, aggravating the complexation reaction. Here, we present the successful synthesis and characterization of the first heteronuclear PHAT complexes containing variable numbers of photocenters and potential catalytic centers.



## 2. Experimental

### 2.1. *General*

UV-Vis spectra were obtained using a Perkin Elmer Lambda2 spectrometer using a slit width of 2 nm and a scan rate of 480 nm $min^{-1}$. Emission spectra were recorded using a Jasco FP-6200 spectrofluorometer and a Jobin Yvon Horiba FluoroMax-3

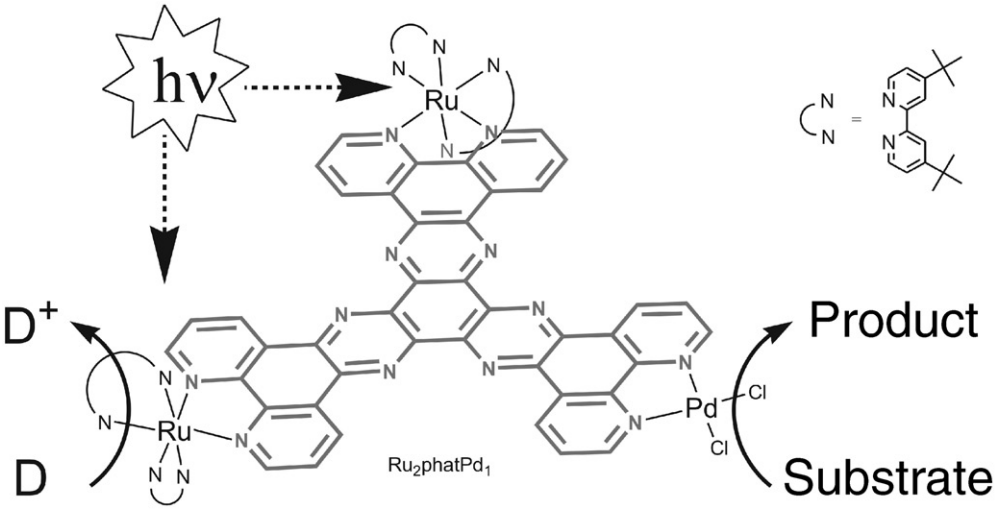


Figure 1. Concept of the supramolecular assembly of **$Ru_2$phat$Pd_1$** [13]. Two single electron-donating chromophores (ruthenium subunits) are connected to a known redox active substructure (palladium center) *via* the bridging ligand PHAT (gray).



spectrometer using a width of excitation and emission slit of 2 nm and an integration time of 0.5 s. Lifetime measurements were obtained using a Jobin Yvon Horiba FlouroLog3 time-correlated, single photon counting apparatus (TCSPC). Excitation occurred with a nanoLED of 467 nm, at a maximum repetition rate of 250 kHz and width of pulse $\leq$200 ps and was detected by Hamamatsu MCP photomultiplier (model R3809U-50, counts: 5000).

NMR spectra were recorded on a Bruker 400 MHz/200 MHz spectrometer and on a Jeol EX-270 DELTA spectrometer (270 MHz), respectively. Mass spectra were recorded with a SSQ 710 spectrometer (Finnigan MAT). Electrospray ionization spectra were recorded with a MAT 95 XL (Thermoquest-Finnigan MAT).

All chemicals were reagent grade and used without purification. Where necessary, all manipulations were carried out using Schlenk techniques under an atmosphere of argon. Prior to use, dichloromethane was distilled over $CaH_2$. Acetonitrile was dried and distilled over molecular sieves A4, methanol was dried and distilled over magnesium. THF, toluene and triethylamine were dried over KOH and distilled over Na/benzophenone. $[Ru(tbbpy)_2Cl_2]$ was purchased from Jena Bioscience. PHAT [11, 15] was prepared according to literature procedures.

Electrochemical data were obtained by cyclic voltammetry using a conventional single-compartment three-electrode cell arrangement in combination with a potentiostat "AUTOLAB®, eco chemie." As auxiliary electrode, a 0.196 $cm^2$ Pt disc was used, while glassy carbon and Ag/AgCl (3 mol $L^{-1}$ KCl) were used as working and reference electrodes, respectively. The measurements were carried out in anhydrous and nitrogen purged ACN with 0.1 mol $L^{-1}$ tetrabutylammonium tetrafluoroborate as supporting electrolyte at ambient temperature (20 ($\pm$5)°C). All potentials are referenced to the ferrocenium/ferrocene couple ($E_{(Fc/Fc+)} = 0.45$ V).

The electronic structure of the molecule was determined applying DFT methods along with the B3LYP hybrid functional [16–18] and the basis set 6-311 G(d,p) [19] using the program package Gaussian 03 [20]. All calculations were performed without symmetry constraints. Population analysis was done employing the NPA method [21].

## 2.2. *Preparation of the metal complexes*

**2.2.1. [{Ru(tbbpy)$_2$}$_3$($\mu$-phat)][PF$_6$]$_6$ (Ru$_3$phat).** Under inert conditions, PHAT (50 mg, 72.4 μmol) and [Ru(tbbpy)$_2$Cl$_2$] (155 mg, 217 μmol) are dispersed in an ultrasonic sound bath in deoxygenated ethylene glycol (250 mL). During 3 h reflux in the microwave (600 W), the violet suspension turned into a clear orange solution. After reducing the solvent to 30–50 mL by microwave distillation, the obtained liquid was filled with water to the starting volume. To precipitate the formed complex $KPF_6$ (240 mg, 1.30 mmol) was added. Filtration and washing with water (five times) gave the crude product, which could be purified by flash chromatography over silica 60 with the solvent mixture acetonitrile : water (ratio 1 : 1/v:v), where the side product [Ru(tbbpy)$_3$][PF$_6$]$_2$ can be removed. Changing the solvent mixture to saturated $KNO_3$ solution : water : acetonitrile (ratio 5 : 30 : 120/v:v:v), the product can be eluted. The purity of the fractions was monitored during workup by TLC ($R_f = 0.8$).

Yield: 200 mg (80%) of brown powder. MS (Micro-ESI in acetonitrile/methanol) $m/z = 434$ (29%) $[M\text{-}6PF_6]^{6+}$, 521 (100%) $[M\text{-}6PF_6]^{5+}$, 651 (59%) $[M\text{-}6PF_6]^{4+}$, and 723 (9%) $[M\text{-}4PF_6]^{4+}$. $^1$H-NMR (400 MHz, $CD_3CN/CF_3COOD$, 300 K): $\delta = 10.22$ (dd, $J = 7.8$ Hz and $J = 1.2$ Hz, 6 H), 8.56 (s, 6 H), 8.522 (s, 6 H), 8.33 (d, $J = 4.8$ Hz, 6 H), 8.12 (dd, $J = 8$ Hz and $J = 5.6$ Hz, 6 H), 7.74 (d, $J = 6.0$ Hz, 6 H), 7.67 (m, 6 H), 7.49 (d, $J = 5{,}6$ Hz, 6 H), 7.36 (m, 6 H), 1.441 (s, 54 H), 1.335/1.327/1.325/1.317 (4s, 54 H) ppm. $^{13}$C{1 H}-NMR (100 MHz, $CD_3CN/CF_3COOD$, 300 K): $\delta = 164.61$, 164.49, 158.66, 155.80, 152.79, 152.57, 152.44, 145.33, 143.23, 135.72, 131.98, 129.22, 126.26, 126.12, 123.00, 36.79, 36.68, 30.80, and 30.69 ppm. UV-Vis (acetonitrile, $c = 12.1 \times 10^{-6}$ mol L$^{-1}$) $\lambda_{max}$ ($\varepsilon$) = 248 (88,000), 258 (90,000), 287 (200,000), 323 (110,000), 368 (69,000), 390 (81,000), 449 (60,000) nm.

**2.2.2. General procedure for preparation of Ru$_3$phat, Ru$_2$phat, and Ru$_1$phat: Method A.** Under argon, PHAT (163 mg, 236 μmol) was dispersed in deaerated ethylene glycol (250 mL) in an ultrasonic sound bath. Under reflux in the microwave (250 W) [Ru(tbbpy)$_2$Cl$_2$] (170 mg, 238 μmol), dissolved in a mixture of ethylene glycol/acetone (85 mL/15 mL), was added dropwise over a period of 9 h. After an additional hour under reflux conditions, the red solution was concentrated to 40 mL and filled with water to the starting volume. After filtration, $NH_4PF_6$ (153 mg, 939 μmol) was added to the product mixture to precipitate the $PF_6$ salt. The red product was filtered off, washed with water five times and dried under vacuum. For separation by flash chromatography, a short column (5–10 cm) with silica 60 as stationary phase was used, eluting with a solvent mixture of acetonitrile : water : saturated $KNO_3$ solution. Starting with the ratio 250 : 30 : 5/v : v : v, the brown fractions [Ru(tbbpy)$_3$][PF$_6$]$_2$ and **Ru$_3$phat** were eluted one after another. After changing the solvent ratio to 155 : 30 : 5/v : v : v for the separation of the **Ru$_2$phat**-fraction, the ratio was changed to 60 : 30 : 5/v : v : v to collect the **Ru$_1$phat** fraction. All fractions were

dissolved in acetonitrile and reprecipitated with $NH_4PF_6$ in water. The ratio of the yields (**$Ru_3$phat** : **$Ru_2$phat** : **$Ru_1$phat**) varies strongly, depending on the speed of the dropwise addition and the volume of solvent. The overall yield of the reaction is 90%.

**Method B:** In ethylene glycol (1 L), PHAT (100 mg, 145 μmol) and $[Ru(tbbpy)_2Cl_2]$ (103 mg, 145 μmol) were suspended in an ultrasonic sound bath. Afterward, the reaction mixture was heated in the microwave (250 W). As soon as the mixture started to reflux (35 min), the reaction was finished. After removal of most of the solvent on the rotary evaporator, the workup is the same as in Method A. The overall yield is 80%.

**2.2.3. [{Ru(tbbpy)$_2$}$_2$(μ-phat)][PF$_6$]$_4$ ($Ru_2$phat): Method A.** Yield: 58 mg (20%).

**Method B:** Yield: 48%. $^1$H-NMR ($CD_3CN$, 400 MHz): 10.583 (dd, $J = 3.8$ Hz, and $J = 0.8$ Hz, 2 H), 10.242 (dd, $J = 8.0$ Hz and $J = 1.0$ Hz, 2 H), 10.195 (dd, $J = 8.0$ Hz, and $J = 1.0$ Hz, 2 H), 9.462 (dd $J = 5.0$ Hz and $J = 1.3$ Hz, 2 H) 8.575–8.539 (m, 6 H), 8.331 (m, 4 H), 8.100 (m, 4 H), 7.738 (m, 2 H), 7.662 (m, 2 H), 7.506 (m, 2 H), 7.249 (m, 2 H), 1.467 (s, 18 H), 1.149 (s, 18 H), 1.348, 1.341, and 1.336 (m, 36 H) ppm. MS (Micro-ESI in acetonitrile/methanol): $m/z = 491$ (8%) $[M\text{-}4[PF_6]]^{4+}$, 655.5 (87%), $[M\text{-}4[PF_6]]^{3+}$, 704.1 (99%) [M-3[PF6]]$^{3+}$, 892.7 $m/z$ (8%) $[M\text{-}4[PF_6]]^{2+}$, 1055.7 (54%), $[M\text{-}3[PF_6]]^{2+}$, and 1128.1 (100%, $[M\text{-}2[PF_6]]^{2+}$). UV-Vis (acetonitrile): $\lambda_{max}$ ($\varepsilon$) = 247 (62,000 L mol$^{-1}$ cm$^{-1}$), 258 (61,000 L mol$^{-1}$ cm$^{-1}$), 287 (139,000 L mol$^{-1}$ cm$^{-1}$), 325 (81,000 L mol$^{-1}$ cm$^{-1}$), 372 (51,000 L mol$^{-1}$ cm$^{-1}$), 393 (60,000 L mol$^{-1}$ cm$^{-1}$), and 448 (35,000 L mol$^{-1}$ cm$^{-1}$) nm.

**2.2.4. [Ru(tbbpy)$_2$(phat)][PF$_6$]$_4$ ($Ru_1$phat): Method A.** Yield: 11 mg (12%).

**Method B:** Yield: 25%. $^1$H-NMR: very wide signals due to π-interaction. MS (Micro-ESI in acetonitrile/methanol): $m/z = 664$ (100%) [M-2[PF6]]$^{2+}$, 1328 (2,3%), [M-2[PF6]]$^+$, and 1473 (0,4%), [M-[PF6]]$^+$. UV-Vis (acetonitrile): $\lambda_{max}$ ($\varepsilon$) = 202 (160,000 L mol$^{-1}$ cm$^{-1}$), 253 (66,000 L mol$^{-1}$ cm$^{-1}$), 186 (110,000 L mol$^{-1}$ cm$^{-1}$), 329 (79,000 L mol$^{-1}$ cm$^{-1}$), 381 (47,000 L mol$^{-1}$ cm$^{-1}$), 402 (53,000 L mol$^{-1}$ cm$^{-1}$), and 450 (23,000 L mol$^{-1}$ cm$^{-1}$) nm.

**2.2.5. [{Ru(tbbpy)$_2$}$_2$(μ-phat){PdCl$_2$}][PF$_6$]$_4$ ($Ru_2$phat$Pd_1$).** Under inert conditions under protection from light, **$Ru_2$phat** (32 mg, 12.5 μmol) and $[PdCl_2(CH_3CN)_2]$ (3.3 mg, 12.7 μmol) were dissolved in dry dichloromethane (15 mL). After stirring for 24 h at RT, the reaction was completed. The solution was filtered, the filtrate was evaporated, and was taken up in acetonitrile and filtered again. After adding water, the brown complex thatprecipitated was filtered, washed with water, and dried in vacuum. Chromatographic workup was done with the solvent mixture acetonitrile : water : saturated $KNO_3$ solution in the ratio 155 : 30 : 5/v : v : v over silica gel 60.

Yield: 30 mg (90%), $^1$H-NMR: many wide signals. MS (Micro-ESI in acetonitrile/methanol): $m/z = 491$ (17.9%) $[M\text{-}PdCl_2\text{-}4[PF_6]]^{4+}$, 655.5 (72.5%) $[M\text{-}PdCl_2\text{-}4[PF_6]]^{3+}$, 983.7 (11.5%) $[M\text{-}PdCl_2\text{-}4[PF_6]]^{2+}$, 691.1 (54.3%) $[M\text{-}2Cl\text{-}4[PF_6]]^{3+}$, 1036.2 (11.8%) $[M\text{-}2Cl\text{-}4[PF_6]]^{2+}$, 701.4 (100%), $[M\text{-}Cl\text{-}4[PF_6]\text{-}4\,H]^{2+}$, and 1055.2 (3.7%) $[M\text{-}Cl\text{-}4[PF_6] + 2\,H]^{2+}$. UV-Vis (acetonitrile): $\lambda_{max}$ ($\varepsilon$) = 208 (170,000 L mol$^{-1}$ cm$^{-1}$), 250 (60,000 L mol$^{-1}$ cm$^{-1}$), 259 (64,000 L mol$^{-1}$ cm$^{-1}$), 287 (140,000 L mol$^{-1}$ cm$^{-1}$),

322 (87,000 L mol$^{-1}$ cm$^{-1}$), 371 (54,000 L mol$^{-1}$ cm$^{-1}$), 393 (68,000 L mol$^{-1}$ cm$^{-1}$), and 448 (36,000 L mol$^{-1}$ cm$^{-1}$) nm.

**2.2.6. [{Ru(tbbpy)$_2$}($\mu$-phat){PdCl$_2$}$_2$][PF$_6$]$_2$ (Ru$_1$phatPd$_2$).** Under inert conditions with protection from light, **Ru$_1$phat** (30 mg, 18.5 μmol) and [PdCl$_2$(CH$_3$CN)$_2$] (9.6 mg, 37.1 μmol) were dissolved in dry dichloromethane (15 mL). After stirring for 24 h at RT, the reaction was finished. The solution was filtered, the filtrate was evaporated, and was taken up in acetonitrile, and filtered again. After adding water, the brown complex that precipitated was filtered, washed with water, and dried in vacuum. Chromatographic workup with preparative TLC was done with the solvent mixture acetonitrile : water : saturated $KNO_3$ solution in the ratio 155 : 30 : 5/v : v : v over silica gel 60.

Yield: 18 mg (48%), $^1$H-NMR: many wide signals. UV-Vis (acetonitrile): 210 (120,000 L mol$^{-1}$ cm$^{-1}$), 251 (43,000 L mol$^{-1}$ cm$^{-1}$), 259 (42,000 L mol$^{-1}$ cm$^{-1}$), 289 (78,000 L mol$^{-1}$ cm$^{-1}$), 334 (sh, 41,000 L mol$^{-1}$ cm$^{-1}$), 395 (31,000 L mol$^{-1}$ cm$^{-1}$), 414 (38,000 L mol$^{-1}$ cm$^{-1}$), and 454 (sh, 15,000 L mol$^{-1}$ cm$^{-1}$) nm.



**2.2.7. Irradiation experiments for hydrogen evolution.** Under inert conditions, **Ru$_2$phatPd$_1$** (700 μg, 260 nmol) was dissolved in a dry mixture of acetonitrile, water, and triethylamine in the ratio of 22 : 11 : 1/v : v : v in a GC vial. Afterwards, the solution was irradiated for up to 18 h with a LED stick ($\lambda = 470$ nm). Probes of the headspace (exactly 3 mL of gas volume) were tested by repeated determination for hydrogen signals by GC.

## 3. Results and discussion

### 3.1. *Synthesis of the ruthenium complexes*

The bridging ligand was synthesized under inert conditions according to literature starting from freshly prepared hexaaminobenzene which was condensed with 1,10-phenanthroline-5,6-dione in a mixture of acetic acid, tetrahydrofuran, and ethanol in 32% yield [12, 15]. For the preparation of the homonuclear ruthenium complexes of PHAT, the [Ru(tbbpy)$_2$Cl$_2$] precursor complex was used [22]. The latter reactions were accomplished under microwave irradiation in suspensions of boiling ethylene glycol due to the great insolubility of the bridging ligand. In the first experiment, a sixfold excess of the ruthenium precursor was used to investigate whether the inner HAT-like coordination spheres coordinate the sterical demanding {Ru(tbbpy)$_2$}$^{2+}$ fragment. The presence of excess precursor compound did not lead to higher substitution. Mass spectroscopy and NMR experiments of the products showed that the ligand would only undergo a threefold substitution at the phenanthroline-like coordination pockets, forming [{Ru(tbbpy)$_2$}$_3$(phat)]$^{6+}$ (**Ru$_3$phat**). The side product could be separated by flash chromatography and was identified by NMR and MS as excess precursor compound.

For the preparation of the mononuclear [Ru(tbbpy)$_2$(phat)]$^{2+}$ (**Ru$_1$phat**) and the dinuclear [{Ru(tbbpy)$_2$}$_2$(phat)]$^{4+}$ (**Ru$_2$phat**) complexes, a different strategy had to be used. The first and second substitution products of the PHAT ligand (**Ru$_1$phat** and **Ru$_2$phat**) are much more soluble in organic solvents than the starting material. To avoid

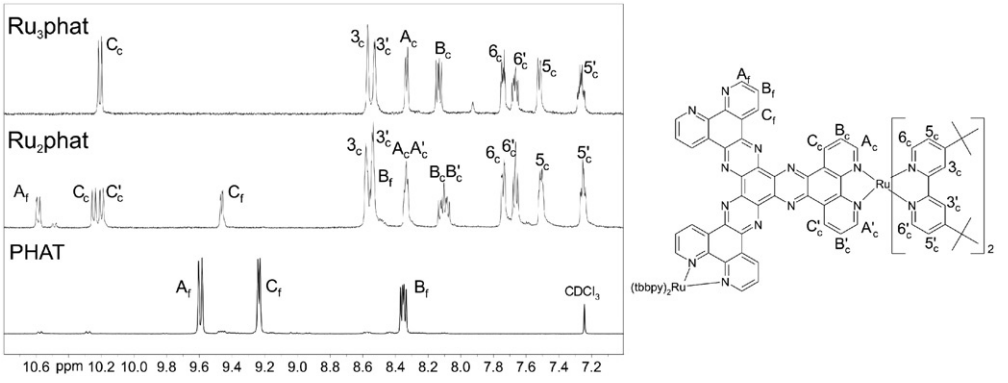


Figure 2. Aromatic region of the NMR spectra of the complexes **$Ru_3$phat** and **$Ru_2$phat** compared to the free ligand PHAT.



their fast complexation, quickly leading to **$Ru_3$phat** during the reaction, a technique created in our group was used [3]. Over 9 h, the precursor complex $[Ru(tbbpy)_2Cl_2]$ was added dropwise to the suspension of PHAT in boiling ethylene glycol during the microwave-heated reaction. The progress of the reaction was monitored by thin layer chromatography, displaying three brown spots, referring to **$Ru_3$phat** eluting in the front followed by **$Ru_2$phat** and **$Ru_1$phat**. After the reaction, the solvent was removed almost completely in vacuum and the hexafluorophosphate salt was precipitated in water. Flash chromatography in acetonitrile : water : saturated $KNO_3$ solution with a solvent gradient gave the $PF_6$ salt of all three complexes, **$Ru_1$phat**, **$Ru_2$phat**, and **$Ru_3$phat** after exchange of the counter ions. After workup, the complexes were identified by NMR and MS experiments. Due to the problems of $\pi$-interaction, some of the NMR spectra had to be taken under the addition of $CF_3COOD$ which has been previously used for related substituted TPPHZ-containing compounds [23]. To show that this procedure would have no effect on the chemical shift, reference spectra of the compound **$Ru_3$phat** were taken in pure $CD_3CN$ and in a mixture of $CD_3CN$ and $CF_3COOD$ in the ratio 100 : 1. Comparison of the NMR spectra showed a pronounced sharpening of the signals and slight shifts of less than 0.1 ppm to lower fields for all peaks in the aromatic region. Detailed analysis of the obtained NMR using HH-COSY allowed identification of the free coordination sphere of the PHAT in **$Ru_2$phat** resonances at 10.58 and 9.46 ppm (figure 2). In addition, a high symmetry of the homotrinuclear complex could be observed.

### 3.2. *Synthesis of the mixed ruthenium palladium species*

In order to form a mixed metal complex that acts as an assembly containing light-harvesting units and catalytically active units, it was necessary to define the positions of the metal centers in the complex. Analogous to the homonuclear complex, it was necessary to investigate whether the $\{PdCl_2\}$ fragment would bind to the inner HAT-like coordination sphere. Therefore, the complex **$Ru_3$phat** was brought to react with $[Pd(CH_3CN)_2Cl_2]$ in the molar ratio 1 : 3 using the standard reaction conditions for this type of reaction [3]. Subsequent analysis of the obtained product by NMR and mass spectroscopy showed only **$Ru_3$phat** signals. Thus, the square planar $\{PdCl_2\}$

fragment is sterically too demanding to allow for coordination at the central HAT positions. For the syntheses of **$Ru_2$phat$Pd_1$** and **$Ru_1$phat$Pd_2$**, the precursor compounds **$Ru_2$phat** and **$Ru_1$phat** were brought to react with $[Pd(CH_3CN)_2Cl_2]$ in dry dichloromethane at ambient temperature in ratios 1 : 1 and 1 : 2, respectively. Inert reaction conditions, exclusion from light, and no heating were used. The reactions were monitored by TLC until they were finished after 24 h. Chromatographic workup proved necessary. Due to the nature of the palladium dichloride fragment coordinated to the bridging ligand, very broad signals in the NMR spectra appeared, making it difficult to interpret.

### 3.3. *Determination of the prepared complexes by mass spectroscopy*

Mass spectroscopy was preferably used for identification and characterization of the multimetal compounds containing palladium, as detailed NMR investigation is precluded by severe signal broadening. Best results could be achieved with the ESI method. In the spectra, generally up to sixfold-charged molecule ions could be detected where only counter ions were lost. Furthermore, in some cases, fragment signals could be assigned in which metal ions were lost during the measurements. This especially counts for the palladium complexes and the $\{PdCl_2\}$ fragment. Comparison of the isotopic pattern of the fragments with the calculated patterns was used for substance identification of all complexes, exemplarily shown in figure 3(a) for **$Ru_2$phat** and in figure 3(b) for **$Ru_2$phat$Pd_1$**.

In conclusion, it is possible to state that modification of a microwave-assisted technique used to synthesize TPPHZ complexes in combination with an optimized workup can be applied successfully to prepare for the first time a series of heteronuclear complexes containing PHAT as bridging ligand, depicted in scheme 1.

### 3.4. *Absorption spectra of the ruthenium/palladium complexes*

The UV-Vis absorption spectra in acetonitrile are shown in figure 4. As observed, for the ruthenium complexes of TPPHZ, the spectra retain most of the features of the components $Ru(tbbpy)_2$ and PHAT. They display the characteristic broad MLCT absorption bands at 400–500 nm attributed to the overlap of the ruthenium orbital with the $\pi^*$ orbitals of TBBPY and PHAT (summarized in table 1). A red shift of the MLCT transition due to coordination to an electron-poor bridging ligand is not observed. Therefore, an increase in the molar extinction coefficient within the series **$Ru_1$phat**, **$Ru_2$phat**, and **$Ru_3$phat** can be observed due to the presence of more ruthenium centers in the supramolecular system. The same effect can be observed for the $\pi \rightarrow \pi^*$ absorption band at 290 nm resulting from additional TBBPY ligands. These observations support the assumption that the chromophore centers, at most, only weakly interact with each other. With increasing number of positively charged ruthenium centers connected to the bridging ligand, a 20 nm hypsochromic shift of the two sharp absorption bands (380 and 405 nm) characteristic of PHAT $n \rightarrow \pi^*$ and PHAT $\pi \rightarrow \pi^*$ transitions to values of about 370 and 390 nm can be observed. Within the heteronuclear complexes, an inverse tendency can be observed. Upon addition of palladium centers to the ruthenium complexes, the PHAT absorption bands are shifted toward lower energies, especially in the case of **$Ru_1$phat$Pd_2$** where the bands appear at 390 and 415 nm. The band at 330 nm is referred to as PHAT $\pi \rightarrow \pi^*$ transition and follows the

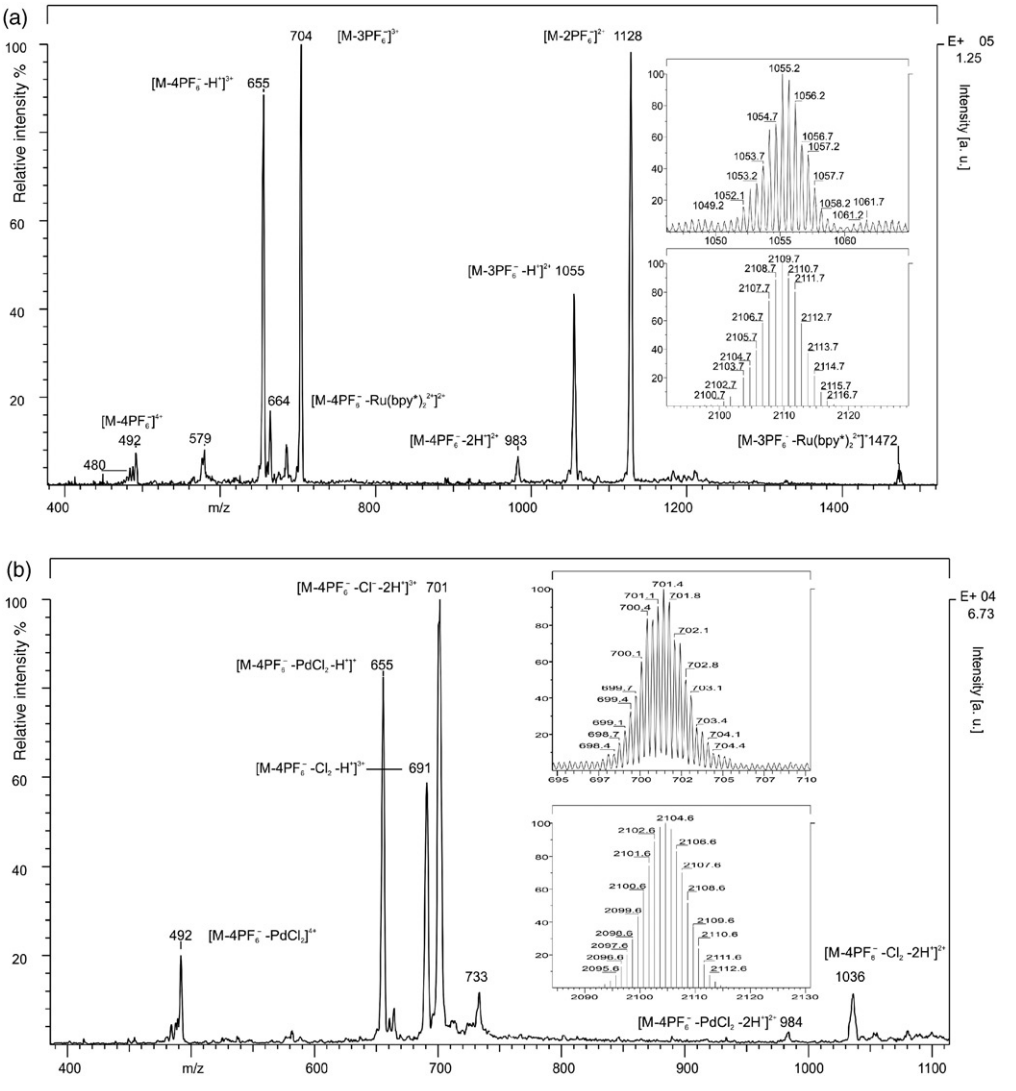


Figure 3. (a). ESI–mass spectra of the complexes **$Ru_2$phat** with isotopic pattern of the predicted and measured mole peak at 1055.2 $m/z$, resulting from the twofold positively charged complex fragment with a molar mass of 2110.4 g mol$^{-1}$, where three $PF_6^-$ and one $H^+$ are lost; (b) ESI–mass spectra of the complexes **$Ru_2$phatPd$_1$** with isotopic pattern of the predicted and measured mole peak at 701 $m/z$, resulting from the threefold positively charged complex fragment with a molar mass of 2070 g mol$^{-1}$, where one chloride, four $PF_6^-$, and two protons are lost.

same tendencies, but due to its pure solubility, the absorption spectra of free PHAT could not be determined and the PHAT-specific absorption bands cannot be assigned precisely yet. The emission spectra of all complexes showed no emission in acetonitrile.

### 3.5. *Cyclic voltammetry of $Ru_3$phat and $Ru_2$phatPd*

**$Ru_3$phat** and **$Ru_2$phatPd$_1$** are the two representative members of the new family of heterooligonuclear PHAT complexes. One is the homometallic ruthenium complex

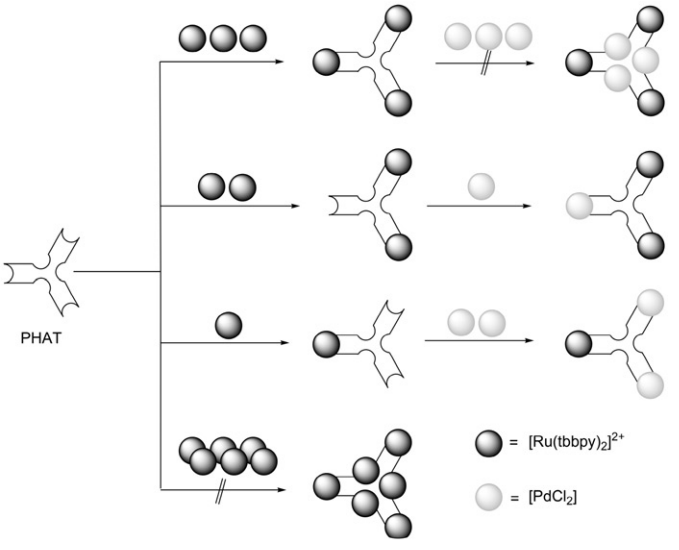


Scheme 1. Overview of the prepared homo- and heteronuclear complexes of the PHAT ligand. Stepwise substitution with {Ru(tbbpy)} fragments (dark gray) leads to formation of the homonuclear series of ruthenium complexes **$Ru_1$phat**, **$Ru_2$phat**, and **$Ru_3$phat**. The first two can be converted to the mixed ruthenium/palladium compounds **$Ru_1$phat$Pd_2$** and **$Ru_2$phat$Pd_1$** by addition of {$PdCl_2$} fragments (light gray) in a second step. Substitution of the inner HAT-like coordination spheres by either of these fragments was not observed.



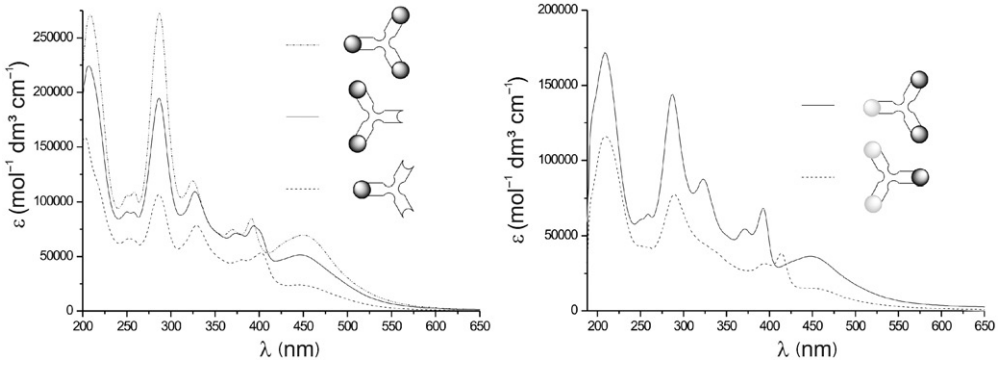


Figure 4. Absorption spectra of the prepared ruthenium complexes (left) and mixed metal complexes (right). All spectra were measured in acetonitrile solution.

which allows us to examine the electrochemical interaction between ruthenium centers and the extended bridging ligand; the other one represents a potential molecular device consisting of two electron-donating chromophores and one electron-accepting metal center, easily reduced. Cyclic voltammetry of the homonuclear and the heteronuclear complexes in $0.1\,\mathrm{mol\,L^{-1}}$ solution of tetrabutylammonium tetrafluoroborate in nitrogen flushed acetonitrile shows the typical $Ru^{2+}/Ru^{3+}$ redox potential at 1.30 V *versus* Ag/AgCl, $3\,\mathrm{mol\,L^{-1}}$ KCl and the typical ligand redox potential of the respective

Table 1. Absorption maxima of the MLCT transition of the prepared compounds.

| Species | Absorption maximum of MLCT (nm) | Extinction coefficient ($Mol\,L^{-1}\,cm^{-1}$) |
|---|---|---|
| **$Ru_3$phat** | 449 | 60,000 |
| **$Ru_2$phat** | 448 | 35,000 |
| **$Ru_1$phat** | 450 | 23,000 |
| **$Ru_2$phat$Pd_1$** | 448 | 36,000 |
| **$Ru_1$phat$Pd_2$** | 454 | 15,000 |

The emission spectra of all complexes showed no emission in acetonitrile.

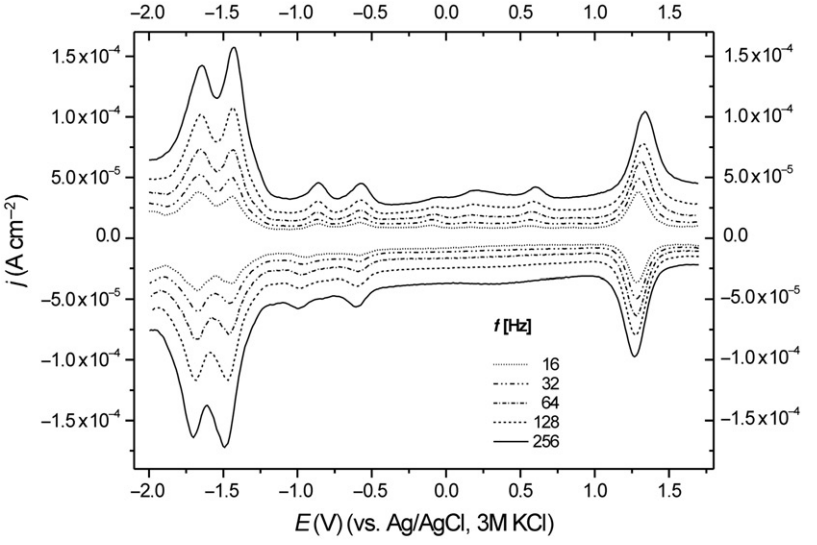


Figure 5. Cyclic voltammetry spectra of the complexes **$Ru_3$phat** in $0.1\,mol\,L^{-1}$ solution of ammonium tetrafluoroborate in acetonitrile at different scan frequencies.

first and second TBBPY ligands of the chromophore subunits at −1.65 and −1.45 V. In the square wave spectra of **$Ru_3$phat** (figure 5 and table 2) additional peaks with a lower intensity can be found at potentials of −0.90 and −0.60 V, which are believed to belong to the bridging ligand. Also, all ruthenium centers are oxidized and reduced at the same potential in the trinuclear complex supports the assumption that no electronic interaction between the PHAT-bridged metal centers is present. In the corresponding region of the **$Ru_2$phat$Pd_1$** square-wave spectra, an irreversible signal appears, see supporting information figure S2. The origin of this irreversible peak can potentially be assigned to the irreversible reduction of the palladium moiety from the complex, which is a known phenomenon for palladium complexes with phenanthroline-like ligands [3].

### 3.6. *Catalytic experiments*

**$Ru_2$phat$Pd_1$** represents the combination of two concepts where one supramolecular system contains two single electron-donating chromophores and one catalytically active

Table 2. Selected redox potentials $E_{1/2}$ (V) of the complexes **$Ru_3$phat**, **$Ru_2$phatPd$_1$**, and $[Ru(tbbpy)_3]^{2+}$ (referenced *vs.* $Fc/Fc^+$ $E_{1/2} = 0.41$ V in a 0.1 mol $L^{-1}$ solution of $Bu_4NBF_4$ in absolute acetonitrile under argon).

| Complex | $L_1$ | $L_2$ | $L_3$ | $L_4$ | $Ru^{2+/3+}$ |
|---|---|---|---|---|---|
| **$Ru_3$phat** | −1.67 | −1.46 | −0.92 | −0.59 | 1.30 |
| **$Ru_2$phatPd** | −1.70 | −1.48 | Irr. | Irr. | 1.28 |
| $[Ru(tbbpy)_3]^{2+}$ | −1.76 | −1.51 | −1.32 | | 1.31 |

Irr., irreversible processes, see supporting information figure S2.



metal interconnected by one bridging ligand capable of multielectron storage. This substance was kept under the standard catalytic conditions used in hydrogen evolution catalyses [3]. In the irradiation apparatus, one probe of the complex **$Ru_2$phatPd$_1$** dissolved in a mixture of water/acetonitrile/triethylamine was irradiated at 470 nm for several hours. The gas phase was analyzed by gas chromatography, but no hydrogen could be detected. During the irradiation of the reaction mixture, a color change from red to green was observed. Therefore, UV-Vis spectra of **$Ru_2$phatPd$_1$** and of all homonuclear ruthenium complexes were taken under catalytic conditions (solvent mixture triethylamine : water : acetonitrile 1 : 11 : 22/v:v:v under argon, irradiation with LEDs $\lambda_{excitation} = 470\,nm \pm 20\,nm$) in isochronous steps. Several different effects could be seen.

During the first 10 min of irradiation of **$Ru_2$phatPd$_1$,** new absorption bands are formed, where all signals increase slightly, forming a ''background absorption'' over the range 400–900 nm. Especially the MLCT band, with its maximum at 450 nm, increases. In comparison, none of the homonuclear ruthenium complexes shows this effect. Nevertheless, the same effect is known for the ruthenium complex with TATPP bridge under similar conditions [9].

After that, under irradiation for 2 h another effect can be seen for **$Ru_2$phatPd$_1$**, depicted in figure 6. Different absorption bands are formed, where all sharp signals most likely associated with the PHAT ligand (325, 375, and 400 nm) disappear, resulting in an unstructured absorption band (figure 6a). During this time also, the MLCT band is lowered, but a new very broad absorption band (500–1000 nm) is formed. In comparison, all homonuclear ruthenium complexes show similar effects (figure 6b). A potential explanation is the destruction of the conjugated $\pi$-system by reduction and protonation of the bridging ligand in this solvent mixture. This behavior has been observed for related ruthenium complexes with TATPP bridges and for dipyridophenazine and its rhenium complexes under similar conditions. The general hypothesis could be checked by chemical reduction of PHAT-containing compounds by spectroelectrochemical investigations. The observed reversibility of the changes in absorption suggests that the chemical changes are reversible as well. We therefore assume that no decomposition occurs [9, 24].

In addition, relaxation processes during a dark phase after short irradiation times can be observed, especially in **$Ru_2$phat**. Here during a dark phase of 10 min and after irradiation for 10 min, the PHAT-associated bands (325, 375, and 400 nm) reappear to give the original spectra. This effect might be explained by intermolecular reactions of the molecule containing the reduced bridging ligand with reactive intermediates in solution, such as recombination reactions with oxidized TEA.

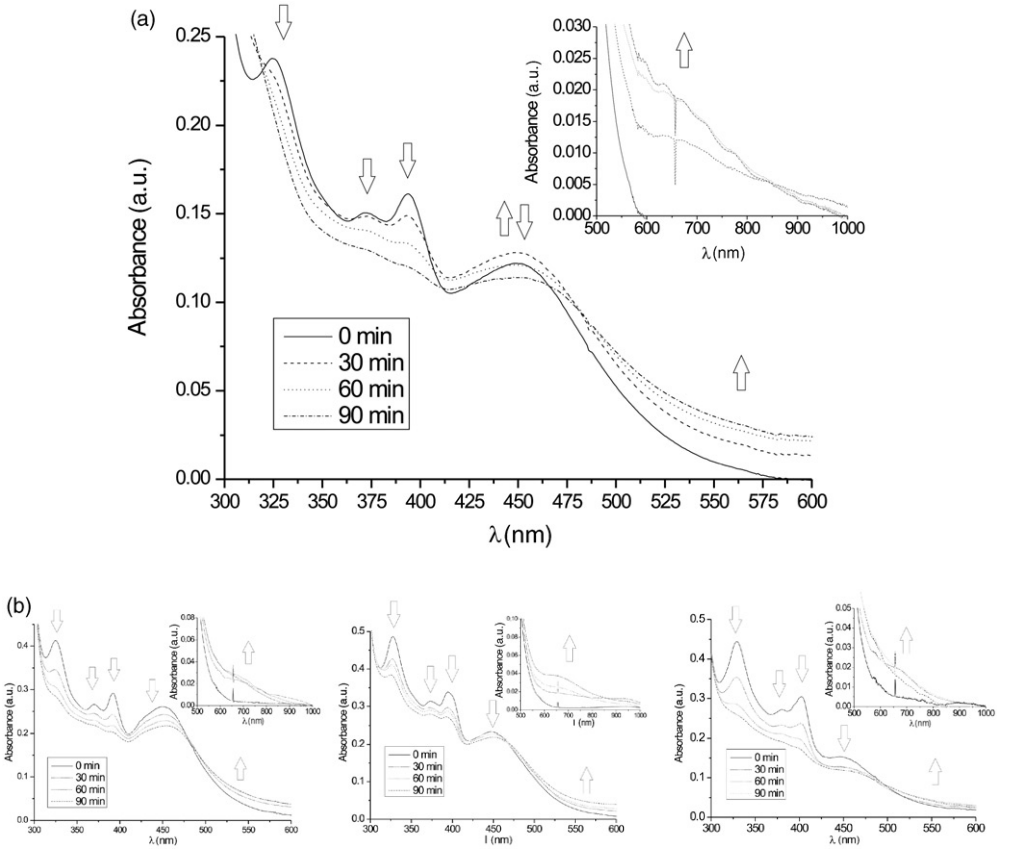


Figure 6. (a). Change of the UV-Vis absorption spectra of **$Ru_2phatPd_1$** in the solvent mixture water : triethylamine : acetonitrile (1 : 11 : 22/v:v:v) under argon during irradiation with blue LEDs ($\lambda_{irradiation} = 470\,nm \pm 20\,nm$) for 90 min; (b) Change of the UV-Vis absorption spectra of **$Ru_3phat$**, **$Ru_2phat$,** and **$Ru_1phat$** in the solvent mixture water : triethylamine : acetonitrile (1 : 11 : 22/v:v:v) under argon during irradiation with blue LEDs ($\lambda_{irradiation} = 470\,nm \pm 20\,nm$) for 90 min.

Nevertheless, the formation of the new species with new absorption band from 500 to 700 nm during long exposition of the complex to visible light is not reversible in the dark phase.

## 4. DFT calculations

Several potential explanations for the lack of catalytic activity could be put forward. A very obvious one would be that the photochemically reduced PHAT molecule consists of non-interacting reduced phenazine-type subunits. If no electron transfer happens within the central HAT core, reduction of the catalytic metal center by the reduced bridging ligand would be very unlikely. In order to obtain some information on this important property, we performed DFT calculations, which have proven very useful for the elucidation of the mechanism in $[Ru(tbbpy)_2(tpphz)PdCl_2]^{2+}$ [3].

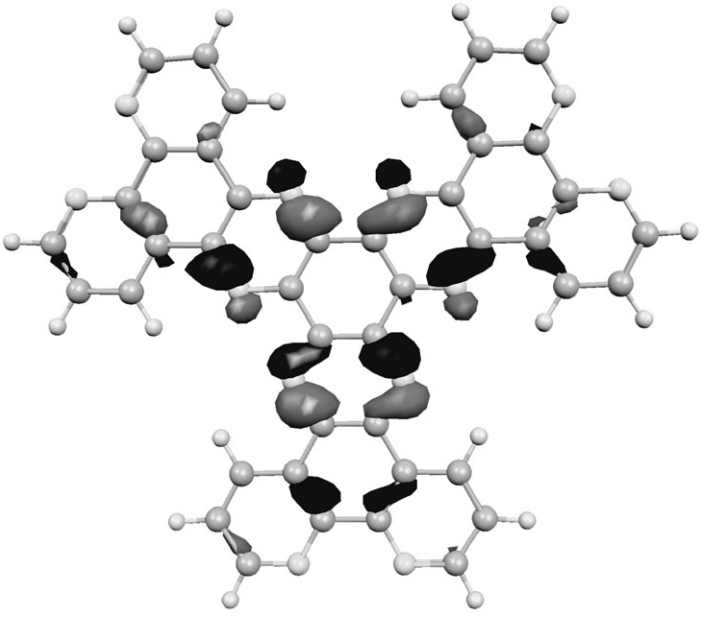

Figure 7. HOMO of the double reduced $PHAT^{2-}$ ion in the singlet state, optimized for gas phase at 0 K.



The preliminary results on the localization of charges in the doubly reduced PHAT molecule are depicted in figure 7. It is clear that the charges are equally distributed over the central HAT core, suggesting an electron delocalization within the central HAT unit. However, in the metal complex, the consideration of additional aspects, such as ground state holes which are present after photoexcitation is necessary. Thus, in the ruthenium complex of PHAT, exciton–exciton annihilation might take place and quench the catalysis. Furthermore, delocalization of electrons within the central HAT core could be disturbed by the coordination of different metal fragments to the phenanthroline sphere. This seems to be rather unlikely taking the observations for $[Ru(tbbpy)_2(tpphz)PdCl_2]^{2+}$ into account, where the electronic properties of the central phenazine nitrogens are hardly influenced by the coordination of a ruthenium core [3, 23]. In **$Ru_2$phat$Pd_1$**, this might not be the case as the redox properties of the HAT core and the Pd subunit might not overlap favorably as observed in the case of TPPHZ complexes. Introduction of a metal center, easier to reduce would therefore provide a way to circumvent this issue.

## 5. Conclusions

We presented here the first synthesis of heterooligonuclear ruthenium–palladium complexes of PHAT. The established synthetic access together with the known interesting properties of PHAT-based systems already explored by Lehn and MacDonnell will in the future enable the synthesis of multimetallic complexes using

this interesting ligand scaffold. We showed in a first step that we can build up a homologous series of ruthenium complexes of the structure $[\{Ru(tbbpy)_n phat\}]^{2n+}$ ($n = 1, 2, 3$) that has the ability to undergo further complexation reactions on its *n*-3 free phenanthroline-like coordination sites. Complexes with metal ions in the inner HAT-like coordination spheres were not obtained. These ruthenium compounds were converted into the heterometallic trinuclear Ru/Pd complexes depicted in scheme 1. The catalytic activity of these supramolecular assemblies for the hydrogen evolution was tested under the standard catalysis conditions, but no hydrogen evolution could be detected in this experiment. A potential explanation for this finding could be drawn from the preliminary DFT calculations on the doubly reduced PHAT molecule. The delocalization of the charges within the central HAT sphere is apparent, with two important implications for future developments. On the one hand, electron transfer within PHAT systems is not localized to a phenazine-type sphere but involves most likely the full HAT as accepting moiety. On the other hand, delocalization of the negative charges will lower the driving force for reduction of a coordinated metal center. Further studies involving PHAT-based systems should therefore focus on the introduction of catalytically active metal centers which are easier to reduce than $PdCl_2$.



## Acknowledgments

We acknowledge the help of Sven Krieck for the measuring of the CV spectra. This work was funded by the Carl-Zeiss-Stiftung, the Deutsche Bundesstiftung Umwelt and the Deutsche Forschungsgemeinschaft (SFB 436).

## References

[1] M. Elvington, J. Brown, S.M. Arachchige, K.J. Brewer. *J. Am. Chem. Soc.*, **129**, 10644 (2007).
[2] H. Ozawa, M. Haga, K. Sakai. *J. Am. Chem. Soc.*, **128**, 4926 (2006).
[3] S. Rau, B. Schäfer, D. Gleich, E. Anders, M. Rudolph, M. Friedrich, H. Görls, W. Henry, J.G. Vos. *Angew. Chem.*, **118**, 6361 (2006).
[4] M. Kaneko, N. Katakura, C. Harada, Y. Takei, M. Hoshino. *Chem. Commun.*, **27**, 3436 (2005).
[5] V. Balzani, F. Scandola. *Supramolecular Photochemistry*, Horwood, Chichester (1991).
[6] K.J. Brewer, M. Elvington, US 2006/0120954 (2006).
[7] S. Tschierlei, M. Presselt, C. Kuhnt, A. Yartsev, T. Pascher, V. Sundström, M. Karnahl, M. Schwalbe, B. Schäfer, S. Rau, M. Schmitt, B. Dietzek, J. Popp. *Chem. Eur. J.*, **15**, 7678 (2009).
[8] C. Chiorboli, S. Fracasso, F. Scandola, S. Campagna, S. Serroni, R. Konduri, F.M. MacDonnell. *Chem. Commun.*, 1658 (2003).
[9] R. Konduri, H. Ye, F.M. MacDonnell, S. Serroni, S. Campagna, K. Rajeshwar. *Angew. Chem. Int. Ed.*, **41**, 3185 (2002).
[10] V. Balzani, S. Campagna, G. Denti, A. Juris, S. Serroni, M. Venturi. *Acc. Chem. Res.*, **31**, 26 (1998).
[11] K. Wärnmark, O. Heyke, J.A. Thomas, J. Lehn. *Chem. Commun.*, 2603 (1996).
[12] F.M. MacDonnell, M. Kim, K.L. Wouters, R. Konduri. *Coord. Chem. Rev.*, **242**, 47 (2003).
[13] M. Auth, S. Rau. Ger. Offen. DE 102007025424 A1, 1 (2008).
[14] R. Nasielski-Hinkens, M. Benedek-Vamos, D. Maetens, J. Nasielski. *J. Org. Chem.*, **217**, 179 (1981).
[15] T. Ishi-i, K. Yaguma, R. Kuwahara, Y. Taguri, S. Mataka. *Org. Lett.*, **8**, 585 (2006).
[16] A.D. Becke. *J. Chem. Phys.*, **98**, 1372 (1993).
[17] A.D. Becke. *J. Chem. Phys.*, **98**, 5648 (1993).
[18] C. Lee, W. Yang, R.G. Parr. *Phys. Rev. B*, **37**, 785 (1988).
[19] R. Krishnan, J.S. Binkley, R. Seeger, J.A. Pople. *J. Chem. Phys.*, **72**, 650 (1980).

[20] M.J. Frisch, G.W. Trucks, H.B. Schlegel, G.E. Scuseria, M.A. Robb, J.R. Cheeseman, J.A. Montgomery Jr, T. Vreven, K.N. Kudin, J.C. Burant, J.M. Millam, S.S. Iyengar, J. Tomasi, V. Barone, B. Mennucci, M. Cossi, G. Scalmani, N. Rega, G.A. Petersson, H. Nakatsuji, M. Hada, M. Ehara, K. Toyota, R. Fukuda, J. Hasegawa, M. Ishida, T. Nakajima, Y. Honda, O. Kitao, H. Nakai, M. Klene, X. Li, J.E. Knox, H.P. Hratchian, J.B. Cross, V. Bakken, C. Adamo, J. Jaramillo, R. Gomperts, R.E. Stratmann, O. Yazyev, A.J. Austin, R. Cammi, C. Pomelli, J.W. Ochterski, P.Y. Ayala, K. Morokuma, G.A. Voth, P. Salvador, J.J. Dannenberg, V.G. Zakrzewski, S. Dapprich, A.D. Daniels, M.C. Strain, O. Farkas, D.K. Malick, A.D. Rabuck, K. Raghavachari, J.B. Foresman, J.V. Ortiz, Q. Cui, A.G. Baboul, S. Clifford, J. Cioslowski, B.B. Stefanov, G. Liu, A. Liashenko, P. Piskorz, I. Komaromi, R.L. Martin, D.J. Fox, T. Keith, M.A. Al-Laham, C.Y. Peng, A. Nanayakkara, M. Challacombe, P.M.W. Gill, B. Johnson, W. Chen, M.W. Wong, C. Gonzalez, J.A. Pople. *Gaussian 03*, Revision C.02, Gaussian, Inc., Wallingford, CT (2004).
[21] A.E. Reed, L.A. Curtiss, F. Weinhold. *Chem. Rev*., **88**, 899 (1988).
[22] S. Rau, B. Schäfer, A. Grüßing, S. Schebesta, K. Lamm, J. Vieth, H. Görls, D. Walther, M. Rudolph, U.W. Grummt, E. Birkner. *Inorg. Chim. Acta*, **357**, 4496 (2004).
[23] M. Karnahl, S. Tschierlei, C. Kuhnt, B. Dietzek, M. Schmitt, J. Popp, M. Schwalbe, S. Krieck, H. Görls, F.W. Heinemann, S. Rau. *Dalton Trans*., **39**, 2359 (2010).
[24] D.A. McGovern, A. Selmi, J.E. O'Brien, J.M. Kelly, C. Longb. *Chem. Commun*., 1402 (2005).